

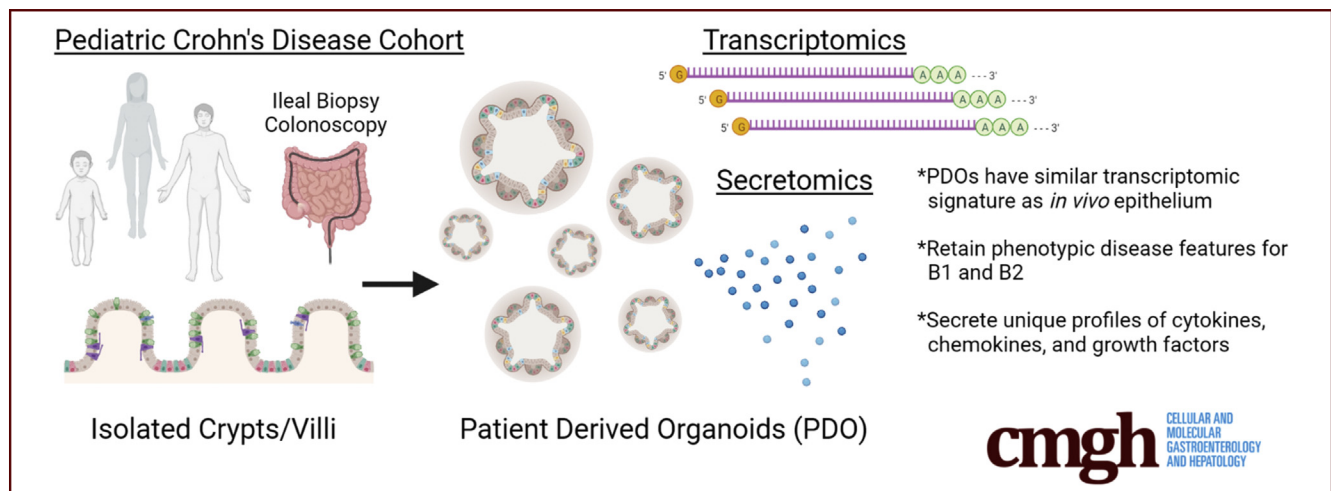
ORIGINAL RESEARCH

Ileal Derived Organoids From Crohn's Disease Patients Show Unique Transcriptomic and Secretomic Signatures



Barbara Joanna Niklinska-Schirtz,¹ Suresh Venkateswaran,¹ Murugadas Anbazhagan,¹ Vasantha L. Kolachala,¹ Jarod Prince,¹ Anne Dodd,¹ Raghavan Chinnadurai,² Gregory Gibson,³ Lee A. Denson,⁴ David J. Cutler,⁵ Anil G. Jegga,⁶ Jason D. Matthews,¹ and Subra Kugathasan¹

¹Division of Pediatric Gastroenterology, Department of Pediatrics, Emory University School of Medicine & Children's Healthcare of Atlanta, Atlanta, Georgia; ²Department of Biomedical Sciences, Mercer University School of Medicine, Savannah, Georgia; ³Department of Biology, Georgia Institute of Technology, Atlanta, Georgia; ⁴Division of Pediatric Gastroenterology, Hepatology, and Nutrition, Cincinnati Children's Hospital Medical Center and the University of Cincinnati College of Medicine, Cincinnati, Ohio; ⁵Department of Human Genetics, Emory University, Atlanta, Georgia; and ⁶Division of Biomedical Informatics, Cincinnati Children's Hospital Medical Center, Department of Pediatrics, University of Cincinnati College of Medicine, Cincinnati, Ohio



SUMMARY

Patient-derived organoids (PDOs) grown from ileal mucosal biopsies can be used to better understand changes in the function of the intestinal epithelium and its role in Crohn's disease. Cultured PDOs show disease-specific signatures at the transcript and secretome level, and we have identified pharmaceutical targets that could potentially reverse these signatures.

BACKGROUND & AIMS: We used patient-derived organoids (PDOs) to study the epithelial-specific transcriptional and secretome signatures of the ileum during Crohn's disease (CD) with varying phenotypes to screen for disease profiles and potential druggable targets.

METHODS: RNA sequencing was performed on isolated intestinal crypts and 3-week-old PDOs derived from ileal biopsies of CD patients (n = 8 B1, inflammatory; n = 8 B2, stricturing disease) and non-inflammatory bowel disease (IBD) controls (n = 13). Differentially expressed (DE) genes were identified by comparing CD vs control, B1 vs B2, and inflamed vs non-inflamed. DE genes

were used for computational screening to find candidate small molecules that could potentially reverse B1 and B2 gene signatures. The secretome of a second cohort (n = 6 non-IBD controls, n = 7 CD, 5 non-inflamed, 2 inflamed) was tested by Luminex using cultured organoid conditioned medium.

RESULTS: We found 90% similarity in both the identity and abundance of protein coding genes between PDOs and intestinal crypts (15,554 transcripts of 19,900 genes). DE analysis identified 814 genes among disease group (CD vs non-IBD control), 470 genes different between the CD phenotypes, and 5 false discovery rate correction significant genes between inflamed and non-inflamed CD. The PDOs showed both similarity and diversity in the levels and types of soluble cytokines and growth factors they released. Perturbagen analysis revealed potential candidate compounds to reverse B2 disease phenotype to B1 in PDOs.

CONCLUSIONS: PDOs are similar at the transcriptome level with the *in vivo* epithelium and retain disease-specific gene expression for which we have identified secretome products, druggable targets, and corresponding pharmacologic agents. Targeting the epithelium could reverse a stricturing phenotype and improve outcomes. (*Cell Mol Gastroenterol Hepatol* 2021;12:1267-1280; <https://doi.org/10.1016/j.jcmgh.2021.06.018>)

Keywords: Inflammatory Bowel Disease; Human Intestinal Organoids; Children; Epigenetics; Intestinal Epithelium; Secretome.

Crohn's disease (CD) is a main form of inflammatory bowel disease (IBD), a heritable chronic inflammatory disorder that can affect the entire gastrointestinal tract. More than 200 genetic susceptibility loci have been found to be associated with CD, of which 90% of the genetic associations are not in the protein coding regions, and heritability was explained by only 15% of affected people having a first-degree relative.¹ For many patients, suppression of inflammation by anti-tumor necrosis factor therapies is currently the primary treatment for CD. However, there are emerging data to support that anti-tumor necrosis factor therapies are effective in controlling the inflammation but not effective in preventing the development of a stricturing phenotype or disease progression, which are the 2 main complications of CD that often require surgical resection.² Even newer biologic therapies offer relief in only a minority of patients. Thus, there is an urgent need for the development of newer treatments targeting different pathways and cell types.

The intestinal epithelium likely plays a pivotal role in the development and disease progression in CD, although the exact mechanisms are not clear.^{3,4} By providing a physical barrier, protecting against foreign microbiota, aiding in nutrient and water absorption, hormone secretion, antigen uptake, and being a mediator of cytokine/chemokine signaling,⁵ any defect in epithelial cell barrier function could have a disastrous consequence on homeostasis. The advent of intestinal organoids from individual patients (patient-derived organoids [PDOs]) allows for the growth of patients' cells in culture from endoscopically derived mucosal biopsies⁶ and has revolutionized IBD research. Intestinal PDOs are three-dimensional structures grown in cell culture that are derived from multipotent epithelial stem cells residing at the base of intestinal crypts. They appear to retain many of the features and functions of the intestinal crypts/epithelium, such as supporting self-renewal, self-organization, barrier function, and differentiation into epithelial cell subtypes (Paneth, Goblet, transit amplifying, etc).⁷ Hence, they provide major advantages compared with epithelial tumor cell lines, primary biopsies, or even animal models.

Herein, we sought to further define the similarities between organoids and intestinal crypts and to test whether CD-specific transcription signatures are retained in PDOs after a short culturing time of 3 weeks and if an epithelial-specific secretome could be measured and used to draw conclusions about disease status. Recently published IBD data suggest that PDOs may lose their inflammatory signature after 5–6 passages,⁸ and thus we sought to investigate an earlier time point. To this end, we analyzed PDO transcriptomes from CD (both stricturing and inflammatory) as well as non-diseased healthy controls and used the changes in these transcription patterns to bioinformatically determine druggable targets for which known pharmacologic compounds are available that could potentially reverse

these CD phenotypes. Our results show that CD-specific transcript signatures are detectable in organoids and suggest that functional changes in the epithelium are potential drivers for CD onset and persistence as observed by changes in soluble cytokine and growth factors produced and released by patient-derived intestinal organoids.


Results

Similar Expression Profiles Exist Between Freshly Isolated Intestinal Crypt Cells and 3-Week-Old PDOs

Manual dissection of ileal mucosal biopsies from pediatric patients yielded intestinal crypt preparations that were used for both RNA sequencing and generation of the organoid cultures (Figure 1A), with typically several hundred organoids per biopsy being produced. Grossly, organoids derived from CD patients look like organoids derived from controls. To confirm the growth of epithelial-specific organoids in our small intestinal crypt culturing system, we immunostained for E-cadherin and lysozyme/Paneth cells (Figure 1B). In addition to staining positive for E-cadherin and lysozyme, these cultures also produced Goblet cells (MUC2 staining, data not shown). During the culturing of organoids, we observed few, if any, differentiating morphologic characteristics between CD and controls after 3 weeks of culture with at least 2 passages (Figure 1C). Occasionally, severely inflamed and friable tissue from CD patients would produce fewer crypts yielding poor growth and subsequent culture failure (~10% of CD cases).

We compared the entire transcriptomic profile (19,900 protein coding genes from hg38) between ileal crypts and corresponding organoids. Of those, we detected 15,554 genes expressed in ileal crypts and/or organoids, and 90.9% of those genes ($n = 14,149$) were expressed in both organoids and crypts. Around 7.0% of the genes ($n = 1091$) were expressed only in ileal crypts, and the remaining 2.0% of genes ($n = 314$) were expressed only in PDOs. We noticed a strong positive correlation in mean expression levels with $R^2 = 0.906$; $P < 10^{-16}$ (Figure 2A) for the genes that are expressed in both ileal crypt and PDOs. Pairwise comparative analysis on entire transcriptomic data of CD and non-IBD controls obtained from both ileal crypts and organoids showed similar patterns between the samples (Figure 2B), consistent with results in Figure 2A. As depicted in Figure 2C, the remarkably similar expression between

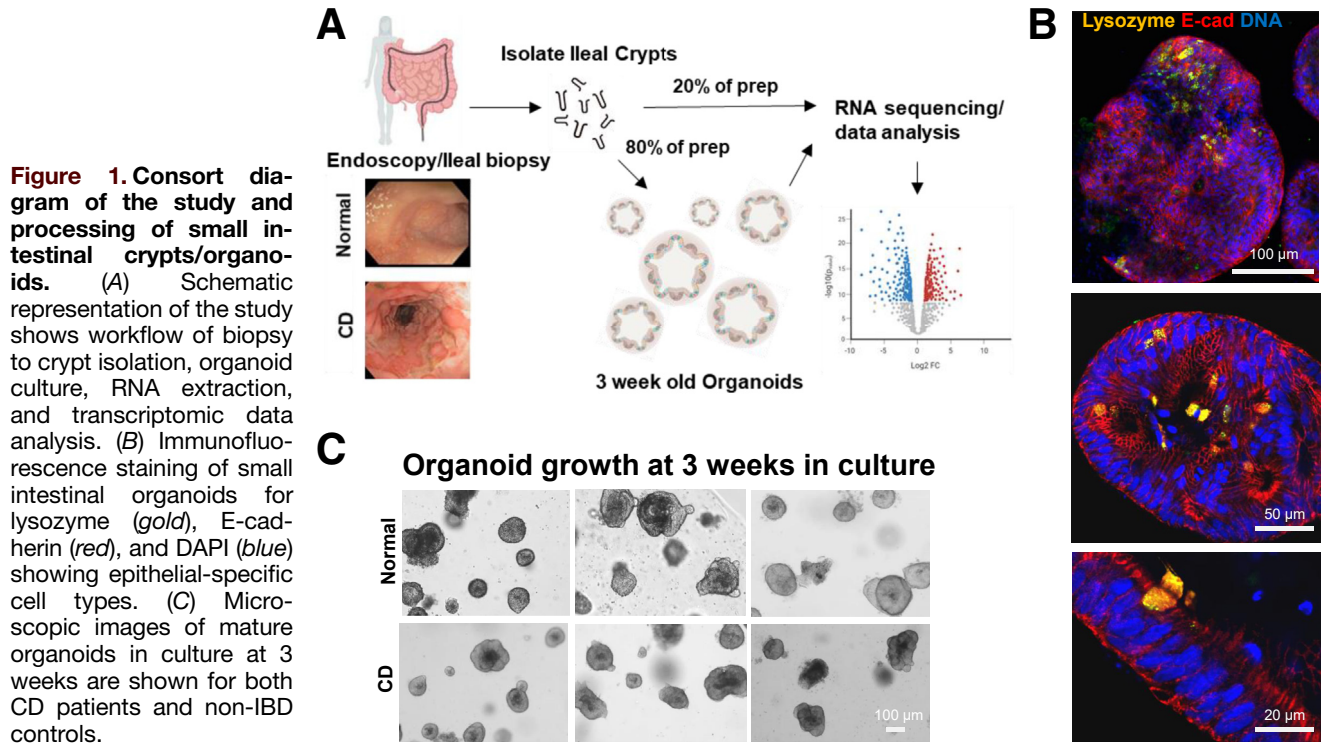
Abbreviations used in this paper: CD, Crohn's disease; DE, differentially expressed; DEG, differentially expressed gene; FC, fold change; FDR, false discovery rate correction; GPCR, G protein-coupled receptor; IBS, inflammatory bowel disease; PBS, phosphate-buffered saline; PCA, principal component analysis; PCR, polymerase chain reaction; PDGF, platelet-derived growth factor; PDO, patient-derived organoid; RIN, RNA integrity number; UC, ulcerative colitis; VEGF, vascular endothelial growth factor.

 Most current article

© 2021 The Authors. Published by Elsevier Inc. on behalf of the AGA Institute. This is an open access article under the CC BY-NC-ND license (<http://creativecommons.org/licenses/by-nc-nd/4.0/>).

2352-345X

<https://doi.org/10.1016/j.jcmgh.2021.06.018>



PDOs and ileal crypt provides evidence that the PDOs are a suitable epithelial model to test druggable targets or measure IBD-specific molecular signatures. Next, we further explored 1091 genes that were expressed only in the ileal crypts using STRING⁹ pathway analysis. This revealed a set of genes that encode proteins involved in immune system signaling/regulation and/or G protein-coupled receptor (GPCR) signaling (Figure 2D). The expression of several protein coding genes involving cellular adhesion was also detected only in the intestinal crypt fraction. Similar analysis for the same genes in Panther pathway¹⁰ revealed the 3 most prominent pathways represented from the “crypt-only” data were (1) inflammation mediated by chemokine and cytokine signaling, (2) heterotrimeric G-protein signaling pathway-Gq alpha and Go alpha pathway, and (3) Wnt signaling.

Disease-Specific Transcriptomic Changes Within PDOs

To examine more subtle differences than gross morphology, we performed differential expression (DE) analysis on bulk RNA sequence data from samples processed as described in Figure 1A, comparing CD organoids with non-IBD control organoids. The analytical representations of the interrogated datasets in principal component (PC) plots, volcano plots, and heatmaps of significantly different transcripts are shown in Figure 3A–C, Supplementary Table 1. The first 2 PCs from the entire transcriptomic profile in PDOs show separation of CD and non-IBD controls along the axis of PC2 ($P = .0046$)

(Figure 3A). The clustering indicates that the PDOs retained a CD-specific gene signature. We performed DE analysis among the disease groups (CD vs non-IBD controls) in PDOs and identified 817 genes to be significantly different at $P < .05$ (Figure 3B). Of the 819 genes, 393 were increased in CD (up-regulated), and 426 were decreased (down-regulated). Consistent with the PC analysis (PCA) in Figure 3A, except for a few CD cases, the hierarchical clustering heatmap identified 2 independent clusters for CD and non-IBD controls using DE genes (DEGs) (Figure 3C). Transcripts encoding several soluble factors were also of interest (Figure 3J). Furthermore, Panther pathway analysis revealed 298 pathway hits, with the top 3 pathways being (1) Wnt signaling, (2) inflammation mediated by chemokine and cytokine signaling, and (3) gonadotropin-releasing hormone receptor pathway. Collectively, our results indicate that the CD-specific transcriptomic profiles were retained in the PDOs after several weeks in culture. It appears that these gene signatures correlate with pathways occurring in non-epithelial cells whose growth is not supported by our culturing conditions. This suggests that disturbances in the crosstalk between non-epithelial mucosal cell types and the epithelium are taking place during IBD, and thus PDOs are reflecting retained defects of the epithelial response to altered extracellular stimulation taking place in the mucosa during CD.

Phenotype-Specific Changes in PDOs From CD

We recently showed the importance of cellular crosstalk in IBD by predicting the progression to stricturing (B2) or

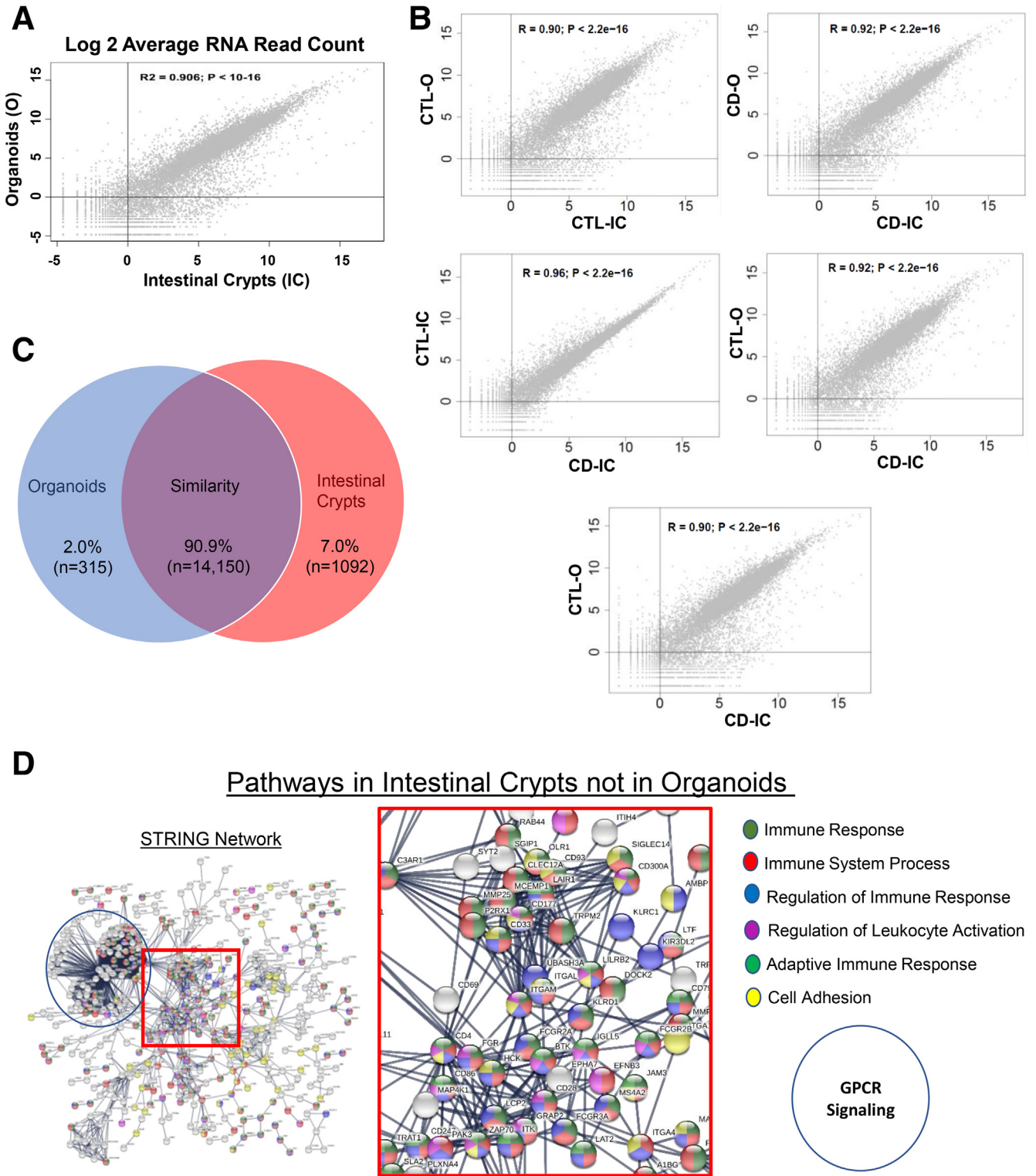


Figure 2. Transcriptomic signatures reveal epithelial nature in PDOs. (A) Scatter plot shows protein coding genes are compared between organoids (X-axis) and ileal crypts (Y-axis). Both X-axis and Y-axis show log transformed average read counts. (B) Pairwise comparison analysis between CD and non-IBD controls for both ileal crypts and organoids. Average read counts for ~20,000 protein coding genes are plotted in each plot. (C) Venn diagram shows number of genes expressed in both organoids and ileal crypts (*purple*), genes that are expressed only in ileal crypts (*blue*), and genes that are expressed only in PDOs (*red*). (D) STRING predicted signaling pathway analysis on the basis of genes that are detected only in ileal crypt preps but not in organoids.

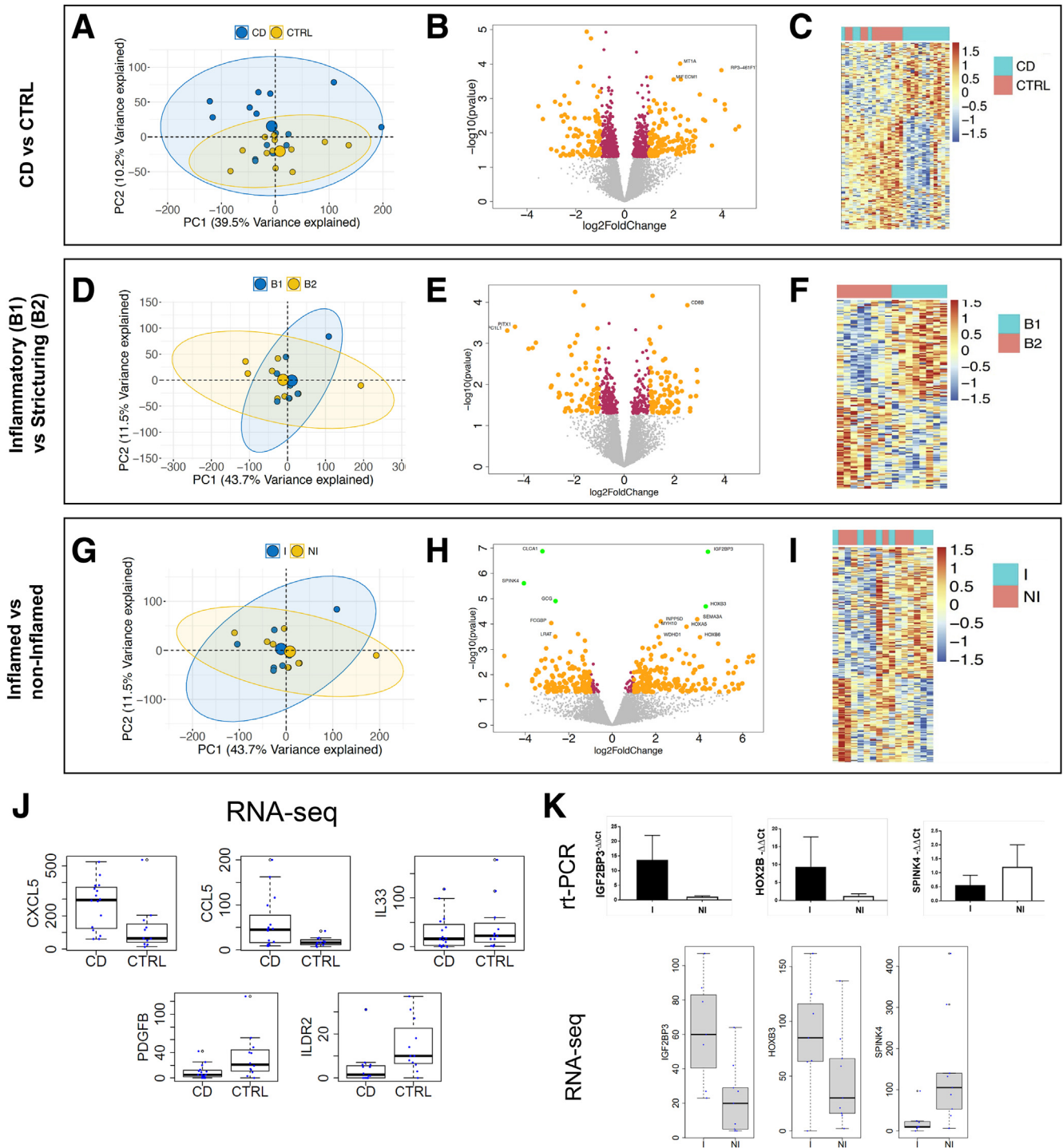


Figure 3. Transcriptomic signatures in PDOs retain disease states. (A) PCA plots with entire transcriptomic data revealed disease-specific expressions (CD vs non-IBD controls). (B) Volcano plot representation on DE results between CD and non-IBD controls show both up- and down-regulated genes. (C) Hierarchical clustering on DEGs shows 2 independent clusters for CD and non-IBD controls. (D) PCA plots with entire transcriptomic data within CD patients not showing any clusters among disease phenotype (B1 and B2). (E) DE analysis between B1 and B2 showed transcriptomic signatures specific to disease phenotypes. (F) Hierarchical clustering on disease phenotype DEGs showed 2 independent clusters. (G) PCA plots with entire transcriptomic data among inflammation status (inflamed and non-inflamed) within CD patients. (H) DE analysis between inflamed and non-inflamed showed transcriptomic signatures specific to inflammation status. (I) Hierarchical clustering on inflammation status specific DEGs showed 2 independent clusters. In PCA plots, the first 2 principal components are plotted along with their variance explained. In volcano plots, the log₂ FCs, log transformed P values are shown on the X-axis and Y-axis, respectively. Maroon indicates the DEGs with $P < .05$, and yellow indicates $P < .05$ and $FC > 1.2$. (J) Box plots comparison between CD versus non-IBD patients shows 5 epithelial-specific genes involved in the innate immune response to be significantly different in PDOs. Y-axis shows the actual read counts. (K) Real-time PCR of IGF2BP3, HOXB2B, and SPINK4 (top) to confirm 3 FDR significant genes between inflamed and non-inflamed CD, as found by RNA sequencing (bottom).

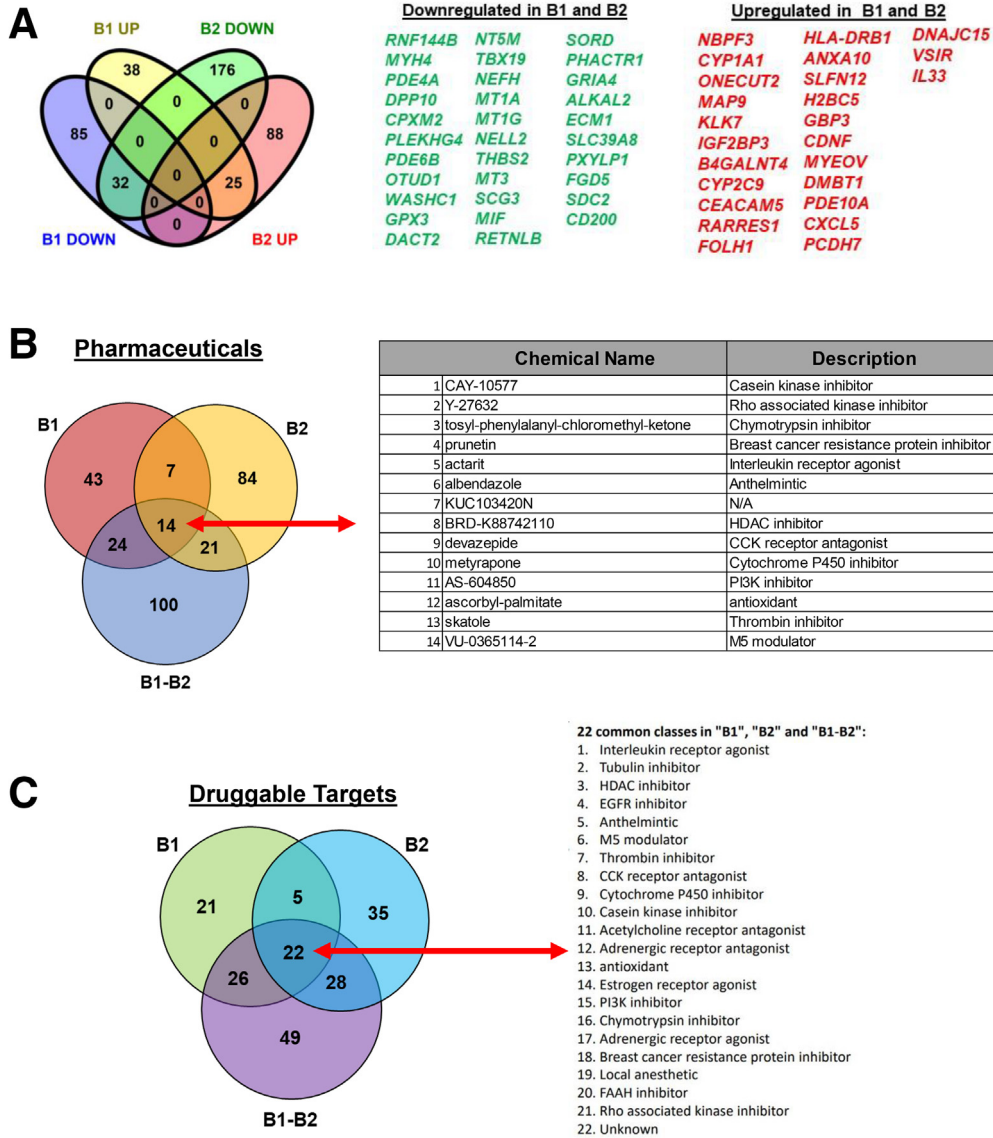


Figure 4. Drug classes and small molecules for B1 and B2 DEGs. (A) Venn diagram shows the DE up- and down-regulated genes that are common among B1 vs non-IBD controls and B2 vs non-IBD controls comparisons. (B) Perturbagen analysis identified small molecules (approved or investigational compounds) belonging to the drug classes outlined in (C). Venn diagram shows number of druggable compounds identified through perturbagen analysis for 3 DEGs sets. List of 14 druggable compounds identified through perturbagen analysis, which is common for 3 DEGs sets and their descriptions. (C) Venn diagram shows number of druggable compound classes identified through perturbagen analysis for 3 DEGs sets. Drug classes (mechanism of action) identified for B1 (B1 vs CTRLs), B2 (B2 vs CTRLs), and shared genes among B1 and B2 DEGs.

penetrating disease (B3) within 3 years of diagnosis.¹¹ The addition of transcriptomic signatures from bulk RNA sequencing data generated from whole ileal biopsies into the analysis significantly improved the accuracy of the risk score. Furthermore, many of the transcription signatures observed to be enriched during B2 in that study belonged to genes involved in extracellular matrix production, most of which are generated by subepithelial myofibroblasts and other non-epithelial cells resident within the lamina propria. Because of our pathway analysis suggesting potential changes in gene expression for soluble molecules such as cytokines, chemokines, and growth factors that regulate the mucosal cellular interactions between the epithelium and lamina propria cells, we further investigated the transcriptional differences that might be contributing to an increase in fibrosis. The use of intestinal PDOs in a growth window where they are still retaining their CD-specific transcription

signature (3 weeks) allowed for strict observation of the transcriptional changes within the epithelium occurring during disease progression early on from B1 to B2 status (Figure 3D–F, Supplementary Table 2). The PCA of the entire transcriptomic profile between B1 and B2 patients did not significantly separate B1 from B2 disease phenotypes (Figure 3D), and the DE analysis between B1 and B2 showed CD phenotype-specific differences in only 470 of 11,933 protein coding genes with $P < .05$ significance, namely fewer than expected by chance. Nevertheless, 156 of these genes had a fold change (FC) >2 (absolute difference in log₂ expression >1), with 83 up-regulated and 73 down-regulated in B1 cultures (Figure 3E). This results in 2 distinct clusters in the heatmap hierarchal clustering for B1 and B2 CD phenotypes DEGs (Figure 3F). Panther pathway analysis on these DEGs identified 188 hits, and the top 3 pathways between B1 and B2 were the same between CD

vs control PDOs but differing in ranking order: (1) gonadotropin-releasing hormone receptor pathway, (2) inflammation mediated by chemokine and cytokine signaling, and (3) Wnt signaling. Thus, the change in chemokine/cytokine differences between B1 and B2, although not formally significant because of the sample size, nevertheless might be related to the onset of signaling leading to changes in extracellular matrix production and the fibrosis observed later in B2/B3 transition.

Inflammation-Specific Changes in PDOs

Finally, we looked at whether the PDO transcriptomic profiles were different within CD patients with respect to inflammatory status (inflamed vs non-inflamed) in the mucosa at endoscopy (Figure 3G-I, Supplementary Table 3). The PCs from the entire transcriptomic profiles do not classify the inflammatory status in the PDOs (Figure 3G). Despite just 358 of 11,933 genes being differentially expressed at $P < .05$, the FCs for this comparison in Figure 3H are much greater than in the above comparisons, suggesting considerable heterogeneity in the expression profiles of the inflamed crypt preparations. A set of 5 genes at or close to experiment-wise significance ($P < 4 \times 10^{-6}$) were significant by false discovery rate correction (FDR) < 0.05 , including increased expression of *IGF2BP3* and *HOXB3* in inflamed PDOs, whereas *CLCA1*, *SPINK4*, and *GCG* were decreased. The hierarchical clustering of DEGs in the heatmap confirmed the substantial heterogeneity between the 2 groups (Figure 3I). Panther pathway analysis on DEGs identified 121 hits, with the platelet-derived growth factor (PDGF) signaling pathway being the most represented within the data, followed by 2 pathways with equal ranking for second highest (angiogenesis and CCKR signaling), followed by 7 pathways in third of which dopamine receptor mediated signaling, inflammation mediated by chemokine and cytokine signaling, and integrin signaling were included. We used a second method to confirm these RNA sequencing observations, and the quantitative polymerase chain reaction (PCR) assays using Taqman primers for *SPINK4*, *IGF2BP3*, and *HOXB3* (Figure 3K) substantiated these findings.

Small Molecules Likely to Reverse B1 and B2 Gene Signatures

We asked whether it was possible to computationally predict, on the basis of known small molecules (approved drugs and investigational compounds) transcriptomics data,¹² candidate therapeutics that might potentially reverse epithelial-specific gene signature observed in B1 and B2 organoids. To perform this, we used 3 sets of DEGs from B1 vs non-IBD controls ($n = 184$ DEGs, Supplementary Table 4), B2 vs non-IBD controls ($n = 323$ DEGs, Supplementary Table 5), and the common genes ($n = 57$ DEGs, Figure 4A) that were consistently up- or down-regulated in both B1 and B2, when compared with controls. We tested all these genes independently against the Touchstone dataset.¹² The perturbation analysis on the 3

DEG sets identified 14 compounds common to all (Figure 4B). The compounds identified for each DE list are provided in Supplementary Table 6. Pathways targeted by the 14 compounds include Rho kinase inhibitor, PI3K inhibitor, interleukin receptor agonist, and cholecystokinin receptor antagonist (Figure 4B). Overall, our analysis identified 14 potential small molecules for 25 of 32 genes that represent the core signature (of B1 and B2), reversal of which could be broadly therapeutic. The summary score reflects the ability of a given small molecule to reverse a disease-specific gene signature. The number of small molecules with the highest scores for therapeutic potential is shown in Figure 4B, and the candidate therapeutics mechanism of action (drug classes or categories) is shown in Figure 4C, whereas the number and corresponding lists are shown in Supplementary Table 6. Experimental validation as well as clinical evaluation will be required to establish whether computational prediction of drug targets using organoid gene expression profiles has presented a new avenue to potentially test the efficacy of old and new pharmaceuticals in reversing the damage of IBD.

Secretome Profiles of Ileal Organoids

Because the pathway analysis of transcriptional differences in the organoids pointed strongly toward changes in cytokines, growth factors, and other soluble molecules released by epithelial cells, we next sought to determine the diversity and levels of secretome released from organoid cultures to further assess any disease-associated characteristics of these samples at the protein level that might functionally impact the behavior of other cell types in the mucosa in a paracrine fashion during CD. The conditioned medium from each organoid culture was collected from a second cohort of CD patients ($n = 6$) and non-IBD controls ($n = 7$, 2 inflamed, 5 non-inflamed; Table 1) and tested by Luminex (Austin, TX) with a 30-analyte panel (Figure 5). The conditioned media from the organoid cultures contained very low levels for many of the analytes including tumor necrosis factor alpha and interferon gamma, even for the inflamed samples. The high levels of epidermal growth factor were the result of its presence in the organoid media for growth purposes. Other molecules in the media produced by PDOs that were readily detectable above baseline levels (we used fresh organoid medium as a negative control for baseline determination) were interleukin (IL) 8 (at high levels), IL15 (moderate levels), and fibroblast growth factor 2 and IL6 (at low levels), but not at statistically significant differences between the CD and controls. However, several of the analytes were detectable at highly variable levels across the samples, and the unique profiles of each patient sample across the 30 analytes appear to have a diagnostic potential. In Figure 5, monocyte chemoattractant protein-1, vascular endothelial growth factor (VEGF), IL8, and IL1RA levels vary considerably across the patient samples and may indicate differences in epithelial health/function between the patients when taken into context with the production and levels of other secretomic signals.

Table 1. Patient Cohort for Organoid Secretome Analysis

Gender	Disease Status	Inflamed/non-inflamed
Male	Control	Non-Inflamed
Male	Control	Non-Inflamed
Male	Control	Non-Inflamed
Female	Control	Non-Inflamed
Female	Control	Non-Inflamed
Female	Control	Non-Inflamed
Male	Crohn's Disease	Non-Inflamed
Male	Crohn's Disease	Non-Inflamed
Female	Crohn's Disease	Non-Inflamed
Female	Crohn's Disease	Non-Inflamed
Female	Crohn's Disease	Non-Inflamed
Female	Crohn's Disease	Inflamed
Female	Crohn's Disease	Inflamed

NOTE. Age range: 2–19 y; average, 14.3 y.

Discussion

Since the original work of Sato et al,⁶ organoid systems have expanded over the last decade, allowing for genetic and functional ex vivo studies by recapitulating many epithelial cell types and functionalities of the original tissue from which they are derived. The intestinal organoid model has propelled work in cancers such as colorectal, gastroesophageal, and prostate cancer, as well as gastrointestinal diseases such as IBD and celiac disease.^{13–15} Herein, we evaluated the capability of pediatric CD PDOs to retain in vivo and disease-specific transcriptional patterns, evaluated how these features differ across phenotypes, and computationally predicted pharmaceuticals to target the CD-specific differences. We found remarkable similarity between in vivo epithelium and organoids at the transcript level and observed that although CD organoids are not morphologically distinct from non-IBD controls, they do retain many disease-specific transcriptional changes that revealed epithelial-specific pathways and show a diverse, patient-specific secretomic profile, any of which could potentially serve as diagnostic signatures or pharmaceutical targets.

Although many studies have relied on organoids, few studies have compared the in vitro transcript signatures with those of the original in vivo epithelium. Middendorp et al¹⁶ evaluated location-specific intestinal transcriptional patterns in mice organoids and found crypt-derived genes being highly maintained in organoid cultures without location-specific external signals from mesenchyme or luminal content. Fuji et al⁷ recently showed the similarities between fresh human intestinal crypts and organoids; however, the profiles generated in that study were limited by analyzing only a few patient samples. We have expanded on the study by Fuji et al by including more patients, along with disease subtypes, and found consistent results. Our studies demonstrate that most genes expressed in the in vivo epithelium are also represented in the organoid cultures (Figure 2C) and that the 7% of genes found in the

intestinal crypt prep, but not organoids, are likely due to the retention of some immune and mesenchymal components during crypt extraction from mucosal biopsies. VanDussen et al¹⁷ showed that current culturing conditions for intestinal organoids derived from isolated crypt preps grow exclusively epithelial cells despite the initial culture having numerous cell types. However, some of these epithelial-specific gene signatures may be stimulated by mesenchymal/immune crosstalk in the mucosa and are lost during organoid culturing or are part of villi that are not reproduced in organoid cultures. Focusing on the genes found only in the intestinal crypt prep, the inability to detect *FPRI*, *CLDN5* and *8*, or *MUC4* in organoids, which are normally expressed in intestinal epithelial cells, suggests that some down-regulation of genes occur in culture, a similar phenomenon also observed by Fuji et al. However, detection of expressed genes such as *CD4*, *CCL22*, *LY9*, *CCL18*, *TLR7* and *CCL3* suggests the presence of immune cells, whereas *RSPO3*, *MMP10*, and *ADAM19* are indicative of stromal cells that were in the intestinal crypt prep after extraction from a mucosal biopsy. It is unclear how the expression of certain epithelial genes is down-regulated in organoids upon culturing, but it is likely that the loss of crosstalk with other mucosal cell types plays a role. Indeed, Fuji et al found that the addition of insulin-like growth factor 1 and fibroblast growth factor 2 to the culturing medium was required to create a transcription profile in the organoids that aligned even closer with that of fresh crypts. Thus, the lack of ligands in the culturing media that are normally produced by non-epithelial cells in the mucosa may drive the loss of cognate GPCR signaling pathways we observed in organoids during culturing (Figure 2D).

Although there were no clear morphologic characteristics observed between CD and control organoids by gross microscopy (Figure 1C), there were measurable differences at the level of transcript abundance (Figure 3A–C). However, a recent report by Kaline et al⁸ showed that after 1 week in culture, PDOs of inflamed origin lost the majority of their

A

Analytes (Pg/ml)	Control						CD-NI					CD-I		Organoid Media	
	#1	#2	#3	#4	#5	#6	#1	#2	#3	#4	#5	#1	#2	#1	#2
IL-6	24	18	14	31	20	27	26	29	16	29	22	23	26	7	7
MCP-1	64	47	27	88	2363	1715	39	353	27	3032	174	392	320	19	33
IL-15	40	34	28	98	51	59	59	66	32	63	42	39	59	10	32
VEGF	320	205	47	309	137	276	261	292	87	296	381	322	261	3	3
IL-1RA	1498	1375	159	477	387	486	2594	1158	336	557	519	276	243	159	207
IL-8	2960	709	87	828	7800	7800	7800	7800	858	7800	7800	941	7800	3	9
IL-2R	34	21	34	116	46	54	62	62	34	58	39	34	50	19	37
RANTES	291	115	14	42	26	25	25	100	13	26	12	12	32	19	24
FGF2	8	6	8	21	16	15	16	15	11	15	13	6	16	7	10
IL-1b	16	16	17	22	19	19	19	20	16	19	15	18	20	13	19
G-CSF(CSF-3)	82	82	82	189	151	151	148	148	108	151	75	89	148	53	138
IL-10	4	4	5	11	7	7	7	7	4	7	5	5	7	4	7
IL-13	17	19	19	45	25	26	26	30	17	28	21	19	26	13	22
IL-12/IL-23p40	7	5	3	24	9	11	11	12	6	11	8	7	11	10	8
Eotaxin (CCL11)	5	6	6	13	10	10	10	10	6	11	6	5	10	5	9
IL-17A(CTLA-8)	4	4	4	28	24	24	24	24	4	25	4	4	24	3	24
MIP-1a	20	25	29	63	30	32	32	30	33	34	29	29	32	20	32
GM-CSF	2	2	1	7	5	4	5	5	2	10	4	2	5	1	4
MIP-1b	17	17	21	115	33	50	24	33	6	42	6	6	33	17	24
EGF	1913	1913	1913	5740	5740	5740	5740	5740	1913	5740	1913	1913	5740	1913	5740
IL-5	2	2	3	11	9	9	9	9	3	1	3	4	9	0	9
HGF	16	16	3	49	16	16	16	16	16	2	3	16	16	16	16
IFN-g	4	4	4	5	3	3	3	3	4	3	4	4	3	4	3
IFN-a	6	7	7	18	11	11	11	11	8	12	7	8	11	6	11
TNFa	2	2	2	6	2	2	2	2	2	2	2	2	2	1	1
IL-2	12	12	12	28	8	7	7	7	12	10	12	12	7	12	7
IL-7	20	14	17	35	14	14	19	19	17	19	20	20	17	10	17
IP-10	41	3	1	7	6	5	5	7	5	5	0	2	5	3	5
MIG	9	5	5	51	9	9	9	9	9	14	5	9	9	5	4
IL-4	40	40	40	73	59	60	62	62	40	62	40	41	62	39	60

B

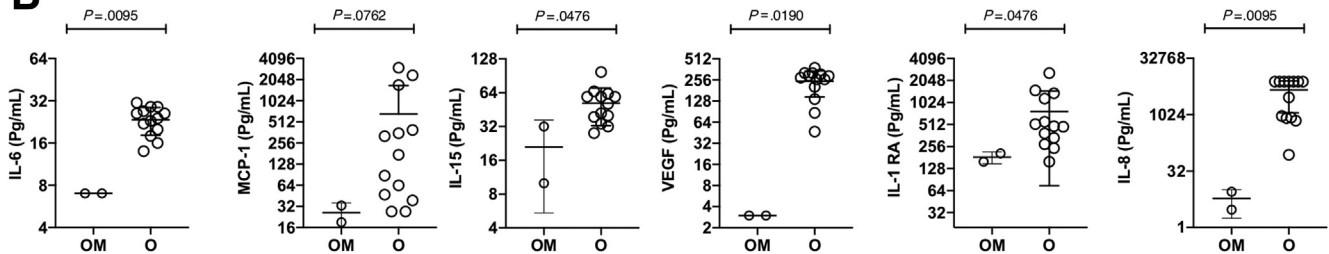


Figure 5. Secretome analysis of PDO conditioned media. Thirty-plex secretome analysis was performed on 3-day-old organoid conditioned media. (A) Concentrations of 30 analytes from the supernatants of Control, Crohn's disease (no inflammation; CD-NI), and Crohn's disease inflammatory (CD-I) organoids are shown. Analyte concentrations in fresh organoid media (background reference) are also shown. Highlighted analytes are statistically significant over the organoid media (background reference). (B) Six of 30 analytes that are significantly higher in organoid condition media (O) over the background Organoid Medium (OM) are shown. Shown results are the cumulative of 2 independent Lumines 30-plex runs.

inflammatory gene expression, but after 4 weeks in culture (5–6 passages) the ulcerative colitis (UC) diseased group remained transcriptionally distinct from non-IBD controls. In contrast to those findings, UC organoids grown for only 1 passage (about 2 weeks) after extraction from mucosal biopsies showed significant differences at the transcript level

when compared with controls.¹⁴ In that study, Dotti et al¹⁴ investigated expression differences that persisted in epithelial organoid cultures generated from patients with UC as compared with non-IBD subjects and found a group of differentially regulated genes in UC patients associated with antimicrobial defenses, as well as secretory and absorptive

functions. Taken together, it appears that many IBD-specific transcriptional changes are retained within organoids at least for some period of time in culture, and these changes likely reflect defective signaling in the gastrointestinal epithelium, perhaps early and distinct, that plays an important role in both forms of IBD onset and progress. In our study, we found a strong signal for inflammatory chemokine and cytokine pathways associated with ileal organoids from CD patients. Finding that a repertoire of soluble factors is being released by the epithelium, some of which differ drastically between patients, substantiates this possibility. Although we did not find group-wide statistical differences between CD and control, the unique signatures for each patient's sample found across the analytes, regardless of phenotype, points toward the disruption of crosstalk that can take place when unique variables are disrupted out of homeostatic alignment. Our method of epithelial-specific profiling of secretomes will allow for a better understanding of mucosal cellular crosstalk as we continue to develop this new protein pipeline and further refine our observations. Our current methodology shows promising potential in elucidating the relationship between gene expression, protein signaling, and cytokine release (secretome) specific to the intestinal epithelium.

In fact, of the 200 epithelial specific genes involved in the innate immune response, we found 5 of the gene transcripts to be markedly different between organoids from CD versus non-IBD patients (Figure 3J). *CXCL5* and *CCL5* transcripts were more abundant in CD, whereas *IL33*, *PDGFB*, and *ILDR2* were found to be less abundant. *CXCL5* is a lipopolysaccharide induced chemokine and an important attractant for immune cell accumulation. It has been studied in various cancers and is increased during IBD, specifically UC patients, indicating a potential role of the epithelium in the regulation of leukocyte migration, general systemic inflammation, and advancement of disease severity in IBD patients.^{18,19} Zhang et al²⁰ recently reported *CXCL5* overexpression as predicting a poor prognosis in pancreatic ductal adenocarcinoma, whereas Nouailles et al²¹ described pulmonary epithelial cells that were secreting *CXCL5* and driving progression of tuberculosis. The increase in *CXCL5* and *CCL5* chemokine transcripts suggests that underlying inflammatory signaling initiated by the epithelium could be playing an important role in driving IBD pathogenesis,²² and although we did not find direct correlation between mRNA levels and extracellular cytokine protein levels, both of these soluble proteins (*CXCL5* and *CCL5*) were detectable in the media of PDOs, along with a number of other proinflammatory and anti-inflammatory cytokines, including *IL8* and *IL1RA*, respectively, and the angiogenic factor *VEGF*.

Indeed, a predominate signature setting the groups of organoids apart was the differential transcription patterns that pointed strongly to immune and angiogenic pathways originating in the epithelium. For example, increases in *CCL5* transcript were up in CD vs controls, and *CX3CL1* transcript was up in B1 vs B2. *CCL5*, also known as *RANTES*, is most commonly reported in human immunodeficiency virus literature and cancers and found to be increased in both UC and CD.^{22,23} Berrebi et al²⁴ also noted that in pediatric

patients with CD, there was an increase of *CCL5* transcript in mucosa within epithelial and immune rich regions, further indicating a role for this cytokine during IBD and the epithelium as a likely source for its production. Remarkably, *PDGF* signaling differed the most between inflamed and non-inflamed samples, which was previously found to be a promising target for anti-fibrotic and anti-angiogenic therapies.²⁵ The role of *PDGF* signaling in IBD is unknown; however, it was increased exclusively in active IBD patients in a small study from Poland.²⁶ We found our CD organoids as a whole exhibit a decrease in *PDGFB* transcript levels and for inflamed samples a decrease in *PDGFA* and *PDGFC* transcript levels, suggesting that the epithelium might also play a role in shaping angiogenic properties associated with IBD.²⁷ The Luminex data support this (Figure 5), because *VEGF* was released at differing levels, suggesting that angiogenic pathways are at play within the epithelium and may reflect changes in crosstalk during CD. Although no differences were found in cytokine transcripts between non-inflamed vs inflamed, *GNG4* was in lower abundance in the inflamed group. Interestingly, *GNG4* is under heavy epigenetic control and is extensively hypermethylated during glioblastoma formation where its expression is down-regulated, leading to a negative impact on the function of GPCRs and chemokine receptors.²⁸ Whether changes in *GNG4* methylation occur in the ileal epithelium during IBD has not been determined, but changes in DNA methylation do occur systemically with increases in inflammation.²⁹ The Wnt pathway is also mediated by GPCR signaling,^{30,31} and changes in transcript levels encoding proteins involved in Wnt pathways were associated with B1 and B2 phenotypes, further indicating defects in pathways requiring crosstalk with non-epithelial cells and the ligands that drive this signaling. When we looked at ways to correct these phenotypes by targeting the most common intersection in physiological changes, our pathway and druggable target analysis found 2 molecules in particular, actarit and devazepide, an IL and CCK receptor blocker (CCK is a GPCR), respectively, that appear to have the most potential in correcting some of the defective signaling observed in the epithelium during CD (Figure 4B).

Conclusion

Overall, our data support PDOs sharing many features at the transcriptome level with the in vivo epithelium and retaining disease-specific phenotypic defects in gene expression. Our process shows that from 2 biopsies, we can generate several hundred PDOs in 2–3 weeks while retaining the disease-specific phenotypes. These PDOs and the conditioned media they generate in culture can be used for further investigations into mechanistic studies of disease progression, particularly structuring and fibrogenesis and potential drug screening. We have identified druggable targets and corresponding pharmacologic agents along with potential endocrine factors originating in the epithelium that may contribute to disease. Many of the pathways shown to be altered in CD are related to immune/non-epithelial crosstalk that is lost upon culturing organoids, suggesting

Table 2. Patient Cohort for Organoid RNA Sequencing Analysis

	CD (N = 16)	Control (N = 12)	Total (N = 28)
Gender			
Female	2 (12.5%)	7 (58.3%)	9 (32.1%)
Male	14 (87.5%)	5 (41.7%)	19 (67.9%)
Age (y)			
Mean (standard deviation)	15.750 (3.215)	11.417 (3.450)	13.893 (3.919)
Range	10.000–20.000	6.000–17.000	6.000–20.000
Disease severity			
B1	8 (50.0%)	NA	8 (50.0%)
B2	8 (50.0%)	NA	8 (50.0%)
Inflammation type			
Inflamed	7 (43.8%)	NA	7 (43.8%)
Non-inflamed	9 (56.2%)	NA	9 (56.2%)
Alignment quality			
Mean (standard deviation)	66.312 (11.578)	74.198 (9.344)	69.692 (11.217)
Range	46.280–79.560	45.550–80.430	45.550–80.430
Aligned number of reads (<i>millions</i>)			
Mean (standard deviation)	7.874 (2.205)	8.068 (1.972)	7.957 (2.072)
Range	4.522–13.189	5.064–12.370	4.522–13.189

that a change in the ability of the intestinal epithelium to perceive and transmit signaling with non-epithelial cells is taking place during CD. It is not clear on the cause of the release of IL8, IL1RA, and VEGF or other cytokines/growth factors from the PDOs during culturing, or whether these differences are measurably different to other patient samples that can better withstand deficiencies in extracellular cues lost during culturing organoids. Thus, more experiments are required to unravel the function of the secretome in these processes. Therefore, future work will begin to interrogate the functional consequences of these differences in transcriptome and secretome and the effects they have on the epithelium and non-epithelial cells in the mucosa.

Methods

Patient Selection and Biopsy Collection

Pediatric patients with CD were recruited for this study after obtaining consent during routine colonoscopy at the Children's Healthcare of Atlanta/Emory University Hospitals from June 2019 through September 2019, and a second cohort was collected between December 2019 and March 2021. In addition, patients undergoing endoscopy for abdominal pain but with grossly normal endoscopies and mucosal biopsies showing normal histology were included as non-IBD controls. In total, 29 mucosal biopsies from 16 CD patients and 13 non-IBD controls were obtained from the terminal ileum by colonoscopy. Table 2 shows patient cohort characteristics used for RNA sequencing analysis. Table 1 contains information on the cohort used in the secretome study. Study design and protocols were approved by the Emory University Institutional Review Board committee. All authors had access to the study data and reviewed and approved the final manuscript. Patients with an established diagnosis of IBD undergoing routine colonoscopies, as well as newly diagnosed CD, were included in the study. Patients with UC or IBD-undetermined were

excluded from the study. CD disease phenotype was determined by Montreal classification with divisions of B1 ($n = 8$, non-stricturing, non-penetrating) and B2 ($n = 8$, stricturing). Patients with B3 (penetrating) phenotype were not included in this study. CD samples were further classified into grossly and microscopically inflamed ($n = 7$) versus non-inflamed ($n = 9$).

Organoid Culture

Two biopsy samples from the terminal ileum per individual were processed. Each sample was exposed to 15 mmol/L EDTA for 45 minutes at 4°C to aid with dissection. Biopsies were manually dissected under stereomicroscopy to extract ileal crypts. Twenty percent of the crypt prep was used for RNA sequencing (stored in RNeasy lysis buffer at -80°C until RNA extraction), and the remaining 80% was used to initiate enteroid cultures. Samples were embedded in Matrigel and overlaid with culture medium (50% Wnt, 20% R-spondin, 10% Noggin conditioned advanced DMEM/F12 medium that included 100 ng/mL EGF, 10 μ mol/L SB202190, 10 nmol/L Leu(15)-Gastrin-1, 2.5 μ mol/L CHIR99021, 0.5 μ mol/L A83-01, 2.5 mmol/L nicotinamide, 1 mmol/L N-acetylcysteine, and 10 μ mol/L Y-27632). Medium was changed every 2–3 days for 3 weeks and passed at least twice before harvesting for RNA extraction. Medium was collected on the third day if used in secretome studies and stored at -80°C.

Immunofluorescence

Organoids grown for 2 or more passages were removed from Matrigel with cold 4% formaldehyde/phosphate-buffered saline (PBS) and fixed for 15 minutes, washed, and then permeabilized with 0.5% Triton X-100/PBS for 15 minutes. Organoids were maintained at room temperature in a liquid suspension within a microfuge tube during permeabilizing and staining, with gentle agitation every 5–10

minutes, and extensive washing between steps (buffer exchanges were performed by a brief centrifugation at 50g to settle organoids and the supernatant removed). Fixed and permeabilized organoids were blocked with 3% bovine serum albumin/PBS and then incubated with primary antibodies (1/250 dilution in blocking buffer) for at least 2 hours (E-cadherin; Sigma-Aldrich, St Louis, MO; lysozyme; Dako Agilent, Santa Clara, CA) and next with secondary antibodies (1/1000 dilution in blocking buffer; goat, anti-rabbit 488, and anti-rat 647 Alexa Fluor conjugates; Thermo Fisher Scientific, Waltham, MA) and DAPI (1/10,000; Thermo Fisher Scientific) for 1 hour. Stained organoids were mounted with Prolong (Thermo Fisher Scientific) between a microscope slide and coverslip and then imaged by confocal microscopy (Olympus FV100; Tokyo, Japan).

RNA Extraction and Sequencing

Total RNA was extracted from intestinal crypts and organoids using a Qiagen (Hilden, Germany) micro-RNA extraction kit and quantified by Nanodrop. RNA integrity numbers (RINs) were determined for samples on a bio-analyzer, and only those samples with RIN values above 7 were sequenced. The library preparation was performed using QuantSeq FWD Kit, a protocol that is designed to generate Illumina (San Diego, CA) compatible libraries of sequences close to the 3' end of polyadenylated RNA. Libraries were sequenced using Illumina NextSeq 550 system by the Molecular Evolution core at Georgia Tech, Atlanta, GA.

Real Time PCR

Total RNA from a subset of patients in [Table 2](#) (inflamed and non-inflamed CD) were tested. First strand cDNA was synthesized with 400 ng of RNA, oligo dTs, and random primers in a final volume of 20 μ L according to the manufacturer's instructions (Thermo Fisher Scientific). Quantitative PCR was performed as a 20 μ L reaction with a final concentration of 1X TaqMan (Thermo Fisher Scientific), 1 μ L of Taqman primer, and cDNA. The reactions were carried out using single step real time PCR machine (Applied Biosystems, Waltham, MA) under the following conditions: initial denaturation at 95°C for 5 minutes, followed by 40 cycles of 2 step amplification at 95°C for 10 seconds and 60°C for 30 seconds. Taqman primers SPINK4, HOXB2, and IGF2BP3, along with RSP01 as the internal control to normalize the RNA levels by delta-delta method, were all obtained from Thermo Fisher Scientific. Two technical repeats and experimental replicates were performed for each gene.

Bioinformatics Analysis

The sequenced raw FastQ files were aligned with reference genome hg38 using the STAR package.³² In total, ~11,500 protein-coding genes were considered with at least 10 read counts in 50% of samples. DE analysis between disease status (CD cases against controls), among CD phenotypes (B1 against B2), and inflammatory status

(CD inflamed against non-inflamed) groups were performed using Deseq2 package³³ after adjusting for age and gender as covariates. The DEGs were identified with $FC \geq 1.2$ and $FDR < 0.05$ or nominal P value $< .05$. *Heatmap* was used to generate the heatmaps for DEGs.³⁴ The PCA was performed with the *prcomp* function, and the PCA plots were generated using the *factoextra* package in R.³⁵

Pathway Analysis

Pathway analysis was performed with STRING⁹ and Panther¹⁰ pathway analysis using differential transcript lists and default settings.

Perturbagen Analysis

To discover potential small molecules likely to reverse B1 and B2 gene signatures, we used the LINCS cloud web tool from the NIH's LINCS Library.¹² We used the small molecule gene-expression signatures from the Touchstone dataset, which has gene expression signatures on 9 distinct cell lines after treatments and includes more than 8000 perturbagens (>2000 small molecules including Food and Drug Administration-approved drugs). The LINCS cloud web tool compares queried signatures with gene expression profiles in the Touchstone library. Compounds whose signatures are anti-correlated to the queried signature are assumed to have a reversing effect and hence may be of therapeutic potential if the queried signature is from a disease state.

Luminex

The used medium from the organoid culture was analyzed for secretome diversity and levels. Supernatants of conditioned organoid media were collected 3 days after a fresh medium change, followed by a brief centrifugation (500g for 5 minutes) and then stored at -80°C. Subsequently, medium supernatants were analyzed by magnetic bead-based multiplex Luminex assays for cytokines, chemokines, and growth factors, including fibroblast growth factor-basic, interferon- γ , IL12 (p40/p70), IL13, CCL5 (regulated on activation, normal T-cell expressed and secreted or CCL5 [RANTES]), CCL3 (MIP-1alpha), CXCL9 (monokine induced by gamma interferon or CXCL9 [MIG]), CCL4 (MIP-1beta), VEGF, IL1b, IL2, IL4, IL5, IL6, IL2R, CCL2 (MCP-1), CCL11 (Eotaxin), IL8, IL10, IL15, IL17, IL1RA, granulocyte-macrophage colony-stimulating factor, granulocyte-colony stimulating factor, epidermal growth factor, HGF, tumor necrosis factor alpha, IL7, CXCL10 (IP-10), and interferon- α (Human Cytokine 30-plex Panel; Life Technologies, Carlsbad, CA), according to the manufacturer's instructions using Luminex xMAP (multi-analyte profiling) technology. Results were plotted as picograms per milliliter.

References

1. Uhlig HH, Muise AM. Clinical genomics in inflammatory bowel disease. *Trends Genet* 2017;33:629–641.

2. Ma C, Moran GW, Benchimol EI, Targownik LE, Heitman SJ, Hubbard JN, Seow CH, Novak KL, Ghosh S, Panaccione R, Kaplan GG. Surgical rates for Crohn's disease are decreasing: a population-based time trend analysis and validation study. *Am J Gastroenterol* 2017; 112:1840–1848.
3. Kaser A, Pasaniuc B. IBD genetics: focus on (dys) regulation in immune cells and the epithelium. *Gastroenterology* 2014;146:896–899.
4. Mokry M, Middendorp S, Wiegerinck CL, Witte M, Teunissen H, Meddens CA, Cuppen E, Clevers H, Nieuwenhuis EE. Many inflammatory bowel disease risk loci include regions that regulate gene expression in immune cells and the intestinal epithelium. *Gastroenterology* 2014;146:1040–1047.
5. Allaire JM, Crowley SM, Law HT, Chang SY, Ko HJ, Vallance BA. The intestinal epithelium: central coordinator of mucosal immunity. *Trends Immunol* 2019; 40:174.
6. Sato T, Stange DE, Ferrante M, Vries RG, Van Es JH, Van den Brink S, Van Houdt WJ, Pronk A, Van Gorp J, Siersema PD, Clevers H. Long-term expansion of epithelial organoids from human colon, adenoma, adenocarcinoma, and Barrett's epithelium. *Gastroenterology* 2011;141:1762–1772.
7. Fujii M, Matano M, Toshimitsu K, Takano A, Mikami Y, Nishikori S, Sugimoto S, Sato T. Human intestinal organoids maintain self-renewal capacity and cellular diversity in niche-inspired culture condition. *Cell Stem Cell* 2018;23:787–793 e6.
8. Kaline A, Bram V, Anabela SR, Severine V, Catherine V, Marc F. Ex vivo mimicking of inflammation in organoids derived from patients with ulcerative colitis. *Gastroenterology* 2020;159:1564–1567.
9. Szklarczyk D, Franceschini A, Wyder S, Forslund K, Heller D, Huerta-Cepas J, Simonovic M, Roth A, Santos A, Tsafou KP, Kuhn M, Bork P, Jensen LJ, von Mering C. STRING v10: protein-protein interaction networks, integrated over the tree of life. *Nucleic Acids Res* 2015;43(database issue):D447–D452.
10. Mi H, Muruganujan A, Ebert D, Huang X, Thomas PD. PANTHER version 14: more genomes, a new PANTHER GO-slim and improvements in enrichment analysis tools. *Nucleic Acids Res* 2019;47:D419–D426.
11. Kugathasan S, Denson LA, Walters TD, Kim MO, Marigorta UM, Schirmer M, Mondal K, Liu C, Griffiths A, Noe JD, Crandall WV, Snapper S, Rabizadeh S, Rosh JR, Shapiro JM, Guthery S, Mack DR, Kellermayer R, Kappelman MD, Steiner S, Moulton DE, Keljo D, Cohen S, Oliva-Hemker M, Heyman MB, Otlej AR, Baker SS, Evans JS, Kirschner BS, Patel AS, Ziring D, Trapnell BC, Sylvester FA, Stephens MC, Baldassano RN, Markowitz JF, Cho J, Xavier RJ, Huttenhower C, Aronow BJ, Gibson G, Hyams JS, Dubinsky MC. Prediction of complicated disease course for children newly diagnosed with Crohn's disease: a multicentre inception cohort study. *Lancet* 2017; 389:1710–1718.
12. Subramanian A, Narayan R, Corsello SM, Peck DD, Natoli TE, Lu X, Gould J, Davis JF, Tubelli AA, Asiedu JK, Lahr DL, Hirschman JE, Liu Z, Donahue M, Julian B, Khan M, Wadden D, Smith IC, Lam D, Liberzon A, Toder C, Bagul M, Orzechowski M, Enache OM, Piccioni F, Johnson SA, Lyons NJ, Berger AH, Shamji AF, Brooks AN, Vrcic A, Flynn C, Rosains J, Takeda DY, Hu R, Davison D, Lamb J, Ardlie K, Hogstrom L, Greenside P, Gray NS, Clemons PA, Silver S, Wu X, Zhao WN, Read-Button W, Wu X, Haggarty SJ, Ronco LV, Boehm JS, Schreiber SL, Doench JG, Bittker JA, Root DE, Wong B, Golub TR. A next generation connectivity map: L1000 platform and the first 1,000,000 profiles. *Cell* 2017;171:1437–1452 e17.
13. Vlachogiannis G, Hedayat S, Vatsiou A, Jamin Y, Fernandez-Mateos J, Khan K, Lampis A, Eason K, Huntingford I, Burke R, Rata M, Koh DM, Tunariu N, Collins D, Hulkki-Wilson S, Ragulan C, Spiteri I, Moorcraft SY, Chau I, Rao S, Watkins D, Fotiadis N, Bali M, Darvish-Damavandi M, Lote H, Eltahir Z, Smyth EC, Begum R, Clarke PA, Hahne JC, Dowsett M, de Bono J, Workman P, Sadanandam A, Fassan M, Sansom OJ, Eccles S, Starling N, Braconi C, Sottoriva A, Robinson SP, Cunningham D, Valeri N. Patient-derived organoids model treatment response of metastatic gastrointestinal cancers. *Science* 2018; 359:920–926.
14. Dotti I, Mora-Buch R, Ferrer-Picon E, Planell N, Jung P, Masamunt MC, Leal RF, Martin de Carpi J, Llach J, Ordas I, Batlle E, Panes J, Salas A. Alterations in the epithelial stem cell compartment could contribute to permanent changes in the mucosa of patients with ulcerative colitis. *Gut* 2017;66:2069–2079.
15. Freire R, Ingano L, Serena G, Cetinbas M, Anselmo A, Sapone A, Sadreyev RI, Fasano A, Senger S. Human gut derived-organoids provide model to study gluten response and effects of microbiota-derived molecules in celiac disease. *Sci Rep* 2019;9:7029.
16. Middendorp S, Schneeberger K, Wiegerinck CL, Mokry M, Akkerman RD, van Wijngaarden S, Clevers H, Nieuwenhuis EE. Adult stem cells in the small intestine are intrinsically programmed with their location-specific function. *Stem Cells* 2014;32:1083–1091.
17. VanDussen KL, Marinshaw JM, Shaikh N, Miyoshi H, Moon C, Tarr PI, Ciorba MA, Stappenbeck TS. Development of an enhanced human gastrointestinal epithelial culture system to facilitate patient-based assays. *Gut* 2015;64:911–920.
18. Singh UP, Singh NP, Murphy EA, Price RL, Fayad R, Nagarkatti M, Nagarkatti PS. Chemokine and cytokine levels in inflammatory bowel disease patients. *Cytokine* 2016;77:44–49.
19. Ostvik AE, Svendsen TD, Granlund AVB, Doseth B, Skovdahl HK, Bakke I, Thorsvik S, Afroz W, Walaas GA, Mollnes TE, Gustafsson BI, Sandvik AK, Bruland T. Intestinal epithelial cells express immunomodulatory ISG15 during active ulcerative colitis and Crohn's disease. *J Crohns Colitis* 2020.
20. Zhang R, Liu Q, Peng J, Wang M, Li T, Liu J, Cui M, Zhang X, Gao X, Liao Q, Zhao Y. CXCL5 over-expression predicts a poor prognosis in pancreatic

- ductal adenocarcinoma and is correlated with immune cell infiltration. *J Cancer* 2020;11:2371–2381.
21. Nouailles G, Dorhoi A, Koch M, Zerrahn J, Weiner J 3rd, Fae KC, Arrey F, Kuhlmann S, Bandermann S, Loewe D, Mollenkopf HJ, Vogelzang A, Meyer-Schwesinger C, Mittrucker HW, McEwen G, Kaufmann SH. CXCL5-secreting pulmonary epithelial cells drive destructive neutrophilic inflammation in tuberculosis. *J Clin Invest* 2014;124:1268–1282.
 22. McCormack G, Moriarty D, O'Donoghue DP, McCormick PA, Sheahan K, Baird AW. Tissue cytokine and chemokine expression in inflammatory bowel disease. *Inflamm Res* 2001;50:491–495.
 23. Ansari N, Abdulla J, Zayyani N, Brahma U, Taha S, Satir AA. Comparison of RANTES expression in Crohn's disease and ulcerative colitis: an aid in the differential diagnosis? *J Clin Pathol* 2006;59:1066–1072.
 24. Berrebi D, Banerjee A, Paris R, Potet F, Aigrain Y, Emilie D, Cezard JP, Hugot JP, Navarro J, Peuchmaur M. In situ Rantes and interferon-gamma gene expression in pediatric small bowel Crohn's disease. *J Pediatr Gastroenterol Nutr* 1997;25:371–376.
 25. Paniagua RT, Robinson WH. Imatinib for the treatment of rheumatic diseases. *Nat Clin Pract Rheumatol* 2007;3:190–191.
 26. Krzystek-Korpacka M, Neubauer K, Matusiewicz M. Platelet-derived growth factor-BB reflects clinical, inflammatory and angiogenic disease activity and oxidative stress in inflammatory bowel disease. *Clin Biochem* 2009;42:1602–1609.
 27. Alkim C, Alkim H, Koksar AR, Boga S, Sen I. Angiogenesis in inflammatory bowel disease. *Int J Inflamm* 2015;2015:970890.
 28. Pal J, Patil V, Mondal B, Shukla S, Hegde AS, Arivazhagan A, Santosh V, Somasundaram K. Epigenetically silenced GNG4 inhibits SDF1alpha/CXCR4 signaling in mesenchymal glioblastoma. *Genes Cancer* 2016;7:136–147.
 29. Sominen HK, Venkateswaran S, Kilaru V, Marigorta UM, Mo A, Okou DT, Kellermayer R, Mondal K, Cobb D, Walters TD, Griffiths A, Noe JD, Crandall WV, Rosh JR, Mack DR, Heyman MB, Baker SS, Stephens MC, Baldassano RN, Markowitz JF, Dubinsky MC, Cho J, Hyams JS, Denson LA, Gibson G, Cutler DJ, Conneely KN, Smith AK, Kugathasan S. Blood-derived DNA methylation signatures of Crohn's disease and severity of intestinal inflammation. *Gastroenterology* 2019;156:2254–2265 e3.
 30. Schulte G, Wright SC. Frizzleds as GPCRs: more conventional than we thought! *Trends Pharmacol Sci* 2018;39:828–842.
 31. Jiang Y, Zhuo X, Mao CG. protein-coupled receptors in cancer stem cells. *Curr Pharm Des* 2020;26:1952–1963.
 32. Dobin A, Davis CA, Schlesinger F, Drenkow J, Zaleski C, Jha S, Batut P, Chaisson M, Gingeras TR. STAR: ultrafast universal RNA-seq aligner. *Bioinformatics* 2013;29:15–21.
 33. Love MI, Huber W, Anders S. Moderated estimation of fold change and dispersion for RNA-seq data with DESeq2. *Genome Biol* 2014;15:550.
 34. <https://CRAN.R-project.org/package= pheatmap>, 2015.
 35. Kassambara A. Practical guide to principal component methods in R: PCA, M (CA), FAMD, MFA, HCPC, factoextra. *STHDA* 2017;2.

Received September 29, 2020. Accepted June 22, 2021.

Correspondence

Address correspondence to: Subra Kugathasan, MD, Division of Pediatric Gastroenterology, Emory University School of Medicine & Children's Healthcare of Atlanta, 1760 Haygood Drive, W-427, Atlanta, Georgia 30322. e-mail: skugath@emory.edu; fax: (404) 727-4069.

Acknowledgments

The authors thank Shweta Biliya at GA Tech for preparing libraries and performing sequencing. Figure 1A and the graphical abstract were created with BioRender.com.

CRedit Authorship Contributions

Barbara Joanna Niklinska-Schirtz, MD (Conceptualization: Equal; Formal analysis: Equal; Investigation: Equal; Writing – original draft: Lead)
 Suresh Venkateswaran, PhD (Data curation: Lead; Formal analysis: Equal; Software: Lead; Writing – review & editing: Equal)
 Murugadas Anbazhagan, Emory University (Investigation: Equal; Methodology: Equal; Validation: Equal)
 Vasantha L. Kolachala, Emory University (Conceptualization: Equal; Investigation: Equal; Methodology: Equal; Validation: Equal; Writing – review & editing: Supporting)
 Jarod Prince, BS (Methodology: Equal; Project administration: Equal),
 Anne Dodd, BS (Methodology: Equal; Project administration: Equal)
 Raghavan Chinnadurai, Mercer University (Conceptualization: Equal; Formal analysis: Equal; Methodology: Equal; Resources: Lead)
 Gregory Gibson, PhD (Formal analysis: Supporting; Writing – review & editing: Supporting),
 David J. Cutler, PhD (Formal analysis: Supporting; Methodology: Supporting; Writing – review & editing: Supporting),
 Anil G. Jegga, DVM (Formal analysis: Supporting; Investigation: Supporting; Methodology: Supporting; Writing – review & editing: Supporting),
 Lee A. Denson, MD (Methodology: Supporting; Writing – review & editing: Supporting)
 Jason D. Matthews, PhD (Conceptualization: Equal; Formal analysis: Equal; Investigation: Equal; Methodology: Equal; Supervision: Equal; Writing – review & editing: Equal)
 Subra Kugathasan, MD (Conceptualization: Equal; Formal analysis: Equal; Funding acquisition: Lead; Resources: Lead; Supervision: Equal; Writing – review & editing: Equal)

Conflicts of interest

The authors disclose no conflicts.

Funding

Supported in part by NIH (DK89674) and the Marcus Foundation. JDM was in part supported by a career development award from Crohn's and Colitis Foundation CDA#451678. This work was also funded from NIH T32 grant number DK108735-4 for BJN fellowship. Research reported in this publication was supported in part by the Integrated Cellular Imaging shared resource of Winship Cancer Institute of Emory University and NIH/NCI under award number P30CA138292. The content is solely the responsibility of the authors and does not necessarily represent the official views of the National Institutes of Health.